ChemSearch Journal 15(1): 135 – 143, June, 2024
Publication of Chemical Society of Nigeria, Kano Chapter

Received: 26/04/2024 Accepted: 04/06/2024
http://www.ajol.info/index.php/csj

Solvent- Free Synthesis, Characterization, Thermogravimetric and Antimicrobial Studies of Cu(II) Complex with Imine Ligands

[1]*Iorungwa, M. S., [1]Abuh, H., [2]Wuana, R. A., [1]Amua, Q. M., [1]Iorungwa, P. D. and [1]Danat, B. T.

[1]*Inorganic/Physical Chemistry Research Group, Department of Chemistry, Joseph Sarwuan Tarka University, Makurdi, 970001-Nigeria
[2]Department of Environmental Sustainability and Centre for Agrochemical Technology, Joseph Sarwuan Tarka University, Makurdi - Nigeria
***Correspondence Email:** iorungwa.moses@uam.edu.ng

ABSTRACT

Grinding was used as a solvent-free synthetic approach to prepare the ligand (L_1) from 2, 4-Dinitrophenylhydrazine and 3-Hydroxybenzaldehyde with N-(3-hydroxybenzaldehyde)-p-fluoroaniline ligand (L_2) and their Cu(II) complex. Melting point, solubility test, molar conductance, UV-Vis, and IR spectrophotometry were used to characterize these compounds. Thermogravimetric analysis (TGA) was used to investigate the thermal stability of the ligands in conjunction with their Cu(II) complex. Coats-Redfern's approximation methods were used to compute the energy of activation (Ea), entropy of activation (ΔS^o), free energy of activation (ΔG), enthalpy of activation (ΔH^o) and collision frequency (Z). Using scanning electron microscopy (SEM), the surface morphologies of the solid compounds were captured. The particle sizes of the ligands and the metal complex were measured using a particle size analyzer at a diffraction angle of 10.9°. The newly synthesized compounds were screened for their antimicrobial activities. Melting points of the synthesized compounds were in the temperature range of 188 - 194℃ showing that they were fairly stable; solubility in non-polar solvents and molar conductance values ($5.6 – 14.10\ \Omega/cm^{-2}$) indicates that the ligands and the complex are non-electrolytic in nature. Comparing the electronic spectra of the free ligands with that of the complex revealed a shift from lower to higher frequencies which confirmed the chelation of the ligands with Cu(II) ion. The FTIR spectra showed bidentate ligands which coordinated through nitrogen atom of the imine group and the deprotonated oxygen atom of the hydroxyl group. Thermal results of the ligands revealed absence of water crystals while those of the complex showed two molecules of water. The kinetic parameters revealed that the decomposition reactions of these compounds was a first order reaction and the activation energy ($kJmol^{-1}$) were 54.05, 25.59 and 25.95 for HL_1, L_2 and Cu(II) complex respectively, implying that HL_1 require extra energy to form activated complex. The collision frequencies were 7.06×10^{16}, 4.01×10^4 and 7.6×10^4 s^{-1} for HL_1, L_2 and Cu(II) complex, which signifies extra spaces in HL_1 and Cu(II) complex than L_2. Positive values of ΔG of the compounds was an indication that the decomposition was non-spontaneous while positive ΔH^o showed that enthalpy was the driving force for the decomposition process. Negative entropy of activation implied that the degree of disorderliness of the products formed by bonds dissociation was lower than that of the reactants. The Schiff base ligands revealed weak activity against the test bacteria and inactivity against the test fungi while the metal complex significantly increased antimicrobial sensitivity against the test microbes.

Keywords: Antimicrobial, Characterisation, Cu(II) complex, Solvent – free synthesis, Thermogravimetry

INTRODUCTION

Recently, biologically important ligands containing azomethines functional group (-NHN=CH-) are subject of concern for many inorganic chemistry researchers. The interest is attributed to the pharmacological relevance of these organic moieties and their metal complexes as analgesics, anti inflammatory, ulcerogenic, antimicrobial and anticancer agents (Mkpenie *et al.*, 2015) which is dependent on the metal ion, the nature of the ligands and the structure of the complexes (Salvaganapathy and Raman, 2016). These factors partly influence the ability of these complexes to locate the proper target site of activity (Anitha *et al.*, 2011). It is well known that some metal ions can enter cells through their cell walls in the form of complexes, deactivating specific enzymes that ultimately lead to the death of the bacterium. (Slavin *et al.*, 2017). Moreover, earlier studies have demonstrated that the effectiveness of different antimicrobial medicines is frequently increased when they are coordinated with the appropriate metal ion (Patel *et al.*, 2006).

Despite the vast array of antibiotics that are currently accessible for use in medicine, diseases caused by various pathogenic microorganisms continue to spread, and antibiotic resistance is growing. (Aiyelabola *et al*., 2017). Researchers are as a consequence continuously search for new antimicrobial agents. Additionally, earlier studies have also reported that some metal complexes of biologically relevant compounds such as azomethine exhibited promising antimicrobial activities upon chelation (Adkis *et al*., 2000. Metal organic chemistry is becoming an interesting area of research due to the demand of new metal based antimicrobial agents (Moellering, 2011: Terreni *et al*., 2021) as a consequence of antibiotic resistance and the emergence of multidrug-resistant bacteria strains, which are now common and hinders the global control of infectious diseases caused by microorganism.

This work covers the synthesis, characterization, thermal decomposition and antimicrobial activities of Cu^{2+} complex of azomethine (-NHN=CH-).

MATERIALS AND METHODS

Reagents and solvents

Analytical grade reagents purchased from Sigma Aldrich were used as supplied without purification. Salicyaldehyde (≥98.5 %), 2, 4-dinitrophenylhydrazine and 4-fluoroaniline were used in the synthesis of the azomethine ligands, copper(II) chloride (99 %) was used to synthesize the metal complex. Others are glacial acetic acid (≥99.5 %), methanol (≥99.9 %), ethanol (99.8 %), acetone and dimethylsulphoxide (DMSO) (≥99 %) used for solubility test.

Apparatus and Instruments

The apparatus and instruments used were Barnstead electro thermal BI-9100 melting point apparatus with digital thermometer, pH/conductivity series 510 conductivity meters, Perkin Elmer FT-IR spectrophotometer (spectrum BX Model using spectrum version 5.3.1 software), Perkin Elmer spectrophotometer UV-VIS double beam PC scanning spectrophotometer (UVD-2690), using UV-Winlab 2.8.5.04 software version, SB160 heat-stirrer, PW 184 weighing balance, 98-1-B temperature regulating heating mantle, and OV/100/F ovum.

Synthesis of ligand with -NHNCH- (HL_1)

Ligand (HL_1) was prepared by reacting 3-hydroxybenzaldehyde (0.01 mol; 1.22 g) with 2,4-dinitrophenylhydrazine (0.01 mol; 1.98 g) by grinding in a mortar in the presence of 4 drops of water for 10 min. The resultant compound was oven dried at70 °C which yielded 95 % of orange colour microcrystalline compound.

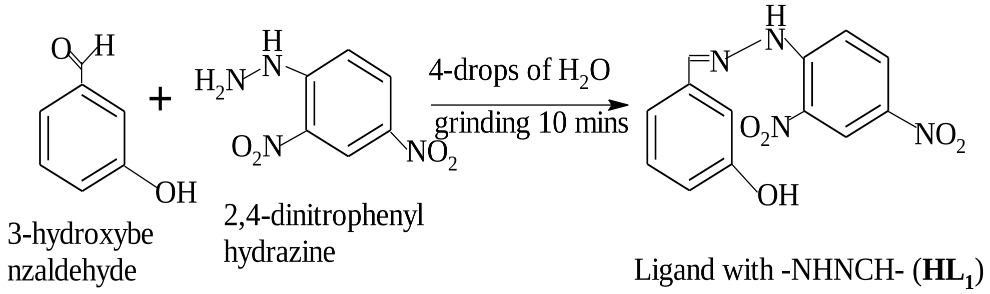

Synthesis of ligand (L_2)

Ligand (L_2) was prepared as described by Ommenya *et al*. (2020) with a few modifications. 4-fluoroaniline (0.3549 g; 0.00319 mol; 0.309 mL) was added to 3-hydroxybenzaldehyde (0.5000 g; 0.00319 mol) in a mortar with 4 drops of water and grinded mechanically with pistol for 10 min, upon which a thick yellowish orange compound was formed. The resulting compound was oven dried at 70 ℃ which formed shiny needle-like yellowish orange crystals.

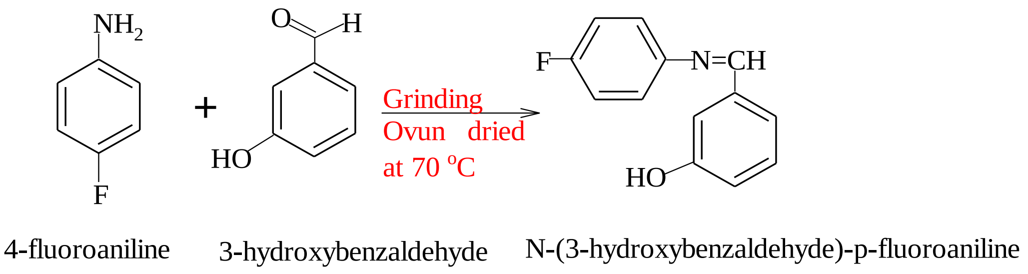

Synthesis of the metal complex containing -NHN=CH- as an active group

Cu(II) complex containing -NHN=CH- as an active group was synthesized by mixing the ligands (0.01 mol of HL_1 and L_2) with the metal(II) salt [0.01 mol of Cu(II) salt] as described by Ommenya *et al*. (2020) in a mortar and ground for 10 min. The resultant compound was oven dried at 70 °C and yielded 97 % of orange coloured microcrystalline Cu(II) complex.

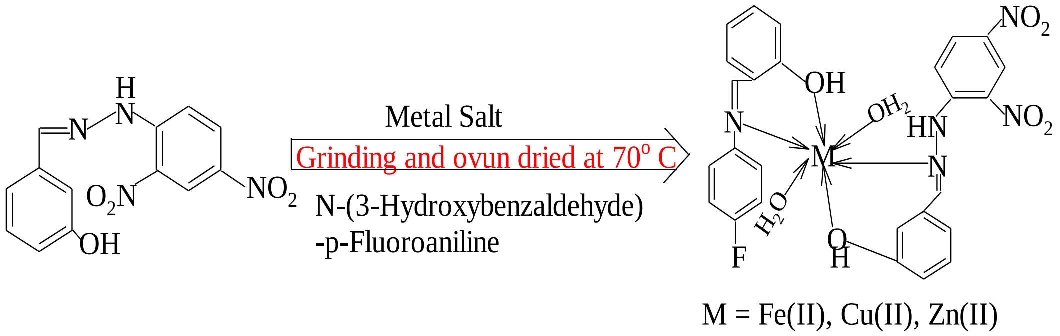

Characterization of the Ligands and its Complex

Solubility test

Exactly 0.01 g of the prepared ligands and its Cu(II) complex were added to 10 mL portions of distilled water, methanol, ethanol, dimethylsulfoxide, dimethylformamide and acetone in separate test tubes and shaken vigorously. A sample is considered soluble if the entire solute dissolves to give a homogenous mixture after shaking. However, if some sample dissolves and some do not, the sample is considered to be slightly soluble and insoluble if the solute remains as introduced (Iniama *et al*., 2018).

Melting point determination

A sample of each of the synthesized compounds was filled in separate capillary tubes to a depth of 2 mm and the bottom tapped several times to ensure close packing. The tube was then inserted into the heating block and heated. The temperature at which each of the samples melted was read from the digital screen and recorded (Subin and Aravindakshan, 2017).

Molar conductivity measurement

The conductivity of the ligands alongside the metal complex was carried out at Rolab Research and Diagonistic Laboratory, Ibadan-Nigeria using Accumet AP75 conductivity meter. Water suspension of 1:5 soil was prepared by weighing 10 g air-dry soil (<2 mm) into a bottle and about 50 mL deionised water was added and shaken mechanically at 15 rpm for 1 h to dissolve soluble salts. The conductivity meter was calibrated according to the manufacturer's instructions using the KCl reference solution to obtain the cell constant. The electrical conductivity of the 0.01M KCl was measured and the conductivity values of ligands and their complexes were recorded as indicated on the conductivity meter.

Infrared and electronic spectra studies

The infrared spectra data of the synthesized metal complex was done in KBr discs and displayed on Perkin Elmer 2000 FT-IR spectrophotometer with spectrum version 5.3.1 software. The ultraviolet spectra of the prepared complexes were obtained using acetone as solvent from Perkin Elmer UVD-2690 UV-VIS double beam PC scanning spectrophotometer (UV-Winlab 2.8.5.04) software version.

Thermogravimetric study

Thermogravimetric study was carried out as described by Emiola-Sadiq *et al*. (2021). TGA of the synthesized compounds were performed using a TG analyzer (TGA-Q50 series, TA instruments) at standard pressure. About 15 mg of each sample was placed in platinum crucibles and heated linearly at six heating rate, 5 °C/min from ambient room temperature to 650 °C. Nitrogen gas at a flow rate of 60 mL/min was used to purge the system and also provided the inert atmosphere for the experiments. The thermograms revealed changes in the structure and other important properties of ligands and metal complexes. From the TG curves, the thermo-kinetic parameters were obtained at the various decomposition temperatures (200, 250, 300, 350 and 400 °C) using Coat-Redfern approximation by plotting $\log\left(ln\frac{W_c/W_r}{T^2}\right)\ Vs\ \left(1/T\right)$which resulted in straight line graphs with slope $\left[-E_a/R\right]$.

Antimicrobial studies

The synthesized ligands and the Cu(II) complex were tested and evaluated for their antimicrobial activity using the agar diffusion technique (Iorungwa *et al.,* 2019). The tested organisms were Gram-negative bacteria (*Escherichia Coli* and *Salmonella typhimurium*), Gram-positive bacteria (*Bacillus subtilis* and *Staphylococcus aureus*). Amoxicillin and nystatin were used as the standard antibacterial and antifugal drugs. The tested bacterial species were grown in Nutrient Agar (NA) medium in petri plates, whereas Sabouraud dextrose agar (SDA) medium was used for fungal species. The media was poured into the sterile petri plates and solidified while the compounds were dissolved in DMF. The inoculum was prepared from the 72 h SDA culture and bacterial species were prepared from a 24 h NA culture. The microbial suspension of each test was evenly spread over the media by sterile cotton swabs. The plates were desiccated and a sterilized cork borer (7 mm in diameter) was used in punching the wells (4 wells) in agar medium. The compounds were then added to the well at different concentration of 25 and 50 mg/ml followed by the diffusion at room temperature for 15 min. The plates were incubated at 37 ℃ for 24 h for bacteria, at 27 ℃ and 72 h for fungi, resulting into the formation of a clear inhibition zone around the well. A meter rule was used in measuring the zone of inhibition. DMF alone was used as a control under the same condition for each organism (El-Barasi *et al*., 2020).

RESULTS AND DISCUSSION

The HL_1, L_2 and Cu(II) complex were all coloured (Table 1) . The ligands and the complex had melting point in the temperature range of 188-194 ºC showing fairly stable ligands and complex compounds. Conductance values were in the range of 5.6 - 14.1 $Ohm^{-1}\cdot m^{-1}$ (Table 1) which were below 50 $Ohm^{-1}\cdot m^{-1}$, indicating their non electrolytic nature (Ommenya *et al*., 2020).

Table 1: Physical Properties of Synthesized Ligands with its Complex

Compound	Colour	Melting Point (ºC)	Conductivity ($Ohm^{-1}m^{-1}$)
HL_1	Orange crystals	190.00	5.6
L_2	Orange-yellow crystals	194.00	5.8
Cu(II) complex	Orange crystals	188.00	14.1

Table 2: Solubility of Ligands along with Complexes at Room Temperature

Compounds	Distilled Water	Methanol	Ethanol	DMF	Acetone	DMSO
HL_1	INS	SS	SS	S	S	S
L_2	INS	SS	SS	S	S	S
Cu(II) complex	INS	SS	SS	S	S	S

Key: S=Soluble SS= slightly soluble INS=Insoluble

Solubility which is one of the characteristic properties of solid compounds gives an idea of their polarity which is used to differentiate them from other compounds and serves as a useful tool in the applications of ligands and their complexes. The ligands and the complex were insoluble in water, slightly soluble in alcohols but soluble in organic solvents like acetone, dimethylsulphoxide (DMSO), dimethylformaldehyde and (DMF) (Table 2). The insolubility of the ligands with the complex in water showed the non-polarity which exists in their structures through covalent and coordinate covalent bond and implies the absence of ionic bond. The insolubility of the complex in water also removes the possibility of counter ions in the complex or that the complex is charged. Solubility of the ligands with the complex improved in organic solvents which could be attributed to the presence of substituents like -OH,-F and $-NO_2$ at the ortho and para positions of the aromatic ring. The nature of the substituent may help improve the solubility of compounds in organic or inorganic media (Das *et al*., 2019).

Table 3: IR Bands (cm^{-1}) of Functional groups for Ligands and its Cu(II) Complex

Compounds	√(N-H)	√(C-OH)	√(C=N)	√(N-N)	√(M-O)	√(M-N)
HL_1	3367	1032	1635	1438		
L_2	3390	1041	1602			
Cu(II) complex	3432	1043	1599	1424	507	425

IR bands at 3367 and 1635 (HL_1), 3390 and 1602 cm^{-1} (L_2) are ascribed to the (–NH) and (C =N) respectively (Table 3). The band at 1032 and 1041 cm^{-1} for HL_1 and L_2 are attributed to C-OH. Also, the IR spectrum of the Cu(II) complex, band for (C = N) is seen at 1599 cm^{-1}. This shift in wave number suggests that coordination of the ligand to the Cu(II) ion was through the (C=N) nitrogen in the ligand. There was no evidence of complexation through the $–NO_2$ group since there was no shift in its band in the metal complex. The new bands in the complex are attributed to the appearance of spectra at 507 cm^{-1} and 425 cm^{-1} which are stretching frequencies of (M–O) and (M–N) bonds respectively (Liu *et al*., 2022).

Table 4: Electronic Spectra Data of the HL_1 and L_2 alongside their Metal Complex

Compounds	λ_{max}**(nm)**	**Assignment**	**Suggested Structure**
HL_1	200.00	$n \rightarrow \pi^*$	
	245.00	$\pi \rightarrow \pi^*$	
	264.00	$\pi \rightarrow \pi^*$	
L_2	205.00	$n \rightarrow \pi^*$	
	213.00	$\pi \rightarrow \pi^*$	
	345.00	$\pi \rightarrow \pi^*$	
Cu(II) Complex	216.00	$n \rightarrow \pi^*$	Tetrahedral
	221.00	$n \rightarrow \pi^*$	
	316.00	$\pi \rightarrow \pi^*$	
	360.00	$\pi \rightarrow \pi^*$	

The Uv-vis spectra of the HL_1, L_2 and Cu(II) complex from 190 to 900 nm exhibited peaks with notable peaks (Table 4). The electronic spectra of HL_1 and L_2 ligands showed prominent absorption bands at (200, 205) nm, assigned to n→π* of C=N and O-hydroxyl group, respectively. Those at (245, 213) nm are assigned to π→π* of C=N azomethine. The third band was at (264, 345) nm, assigned to π→π* of C=C phenyl. The electronic spectra of Cu(II) complex showed four absorption bands of appreciable intensity at (216, 221, 316 and 360) nm assigned to n→π* and π→π* transitions, respectively. These bands suggests an tetrahedral configuration of the Cu(II) complex.

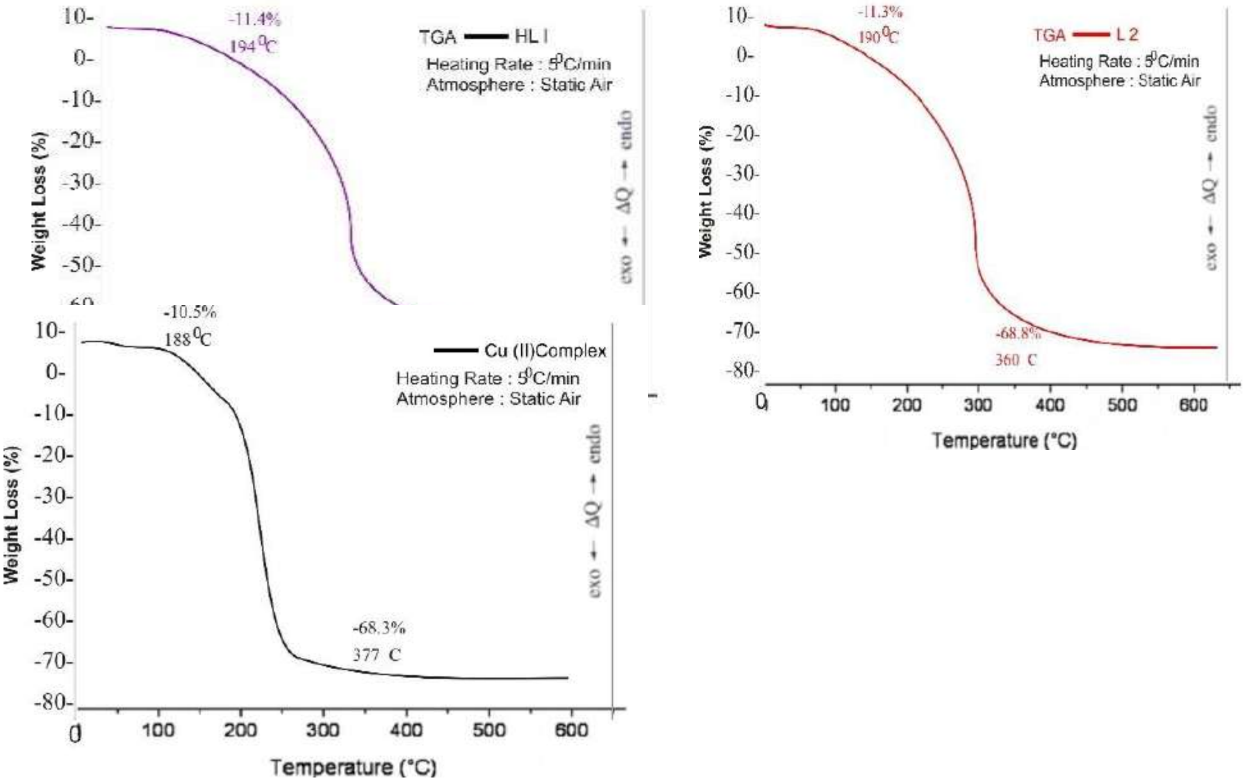

Figures 1a-c: The Themograms of HL_1, L_2 and Cu(II) complex

The thermogram of the Cu(II) complex displayed three-step decomposition process; in the first step 6.0 % weight loss was observed in the range of 39 – 100 ℃, which indicates the presence of two lattice water molecules in the complex. In the second step of decomposition starting from 100 ℃ to 188 ℃, non-chelating part of the ligand was eliminated which represented 10.3 %. In the last step beginning from 188 ℃ to 377 ℃, 68.3 % weight loss was linked to the last part of the ligand and the final pyrolysis product was obtained as Cu(II) oxide of mass 31.7%.

Examining thermograms of HL_1, L_2 along their Cu(II) complex displayed two decomposition steps whereas the complex showed three decomposition steps in the temperature range 0 ℃ to 650 ℃. This variation in the number of steps of decomposition in HL_1, L_2 and the Cu(II) complex confirmed complexation as suggested by the electronic spectra. It was similarly noticed that the thermograms of the ligands and the complex were curved, this demonstrates that the decomposition reactions followed first order kinetics with the gradient of the curves in the order of $\mathbf{L_2}$ <

$\mathrm{Cu(II)complex} < \mathrm{H}\mathbf{L}_1$. This shows the rate of breakdown, which can be explained by the quantity of groups that release or withdraw electrons, which raises or decreases the electron density at the reactive centers and, in turn, increases or decreases thermal stability. (Doğan *et al*., 2020).

Table 5: Thermal Parameters for Non-isothermal Ligands along Complexes by TGA in Air using Coats-Redfern Approximation

Compounds	Kinetics Parameters		Thermodynamics Parameters		
	E_a(kJ/mol)	Z (s^{-1})	ΔH($kJmol^{-1}$)	ΔG ($kJmol^{-1}$)	ΔS($Jmol^{-1}$)
HL_1	54.05	7.06×10^{16}	50.25	20.19	74.10
L_2	25.59	4.01×10^{4}	21.82	98.20	-160.29
Cu(II) Complex	25.95	7.6×10^{4}	22.11	98.22	-156.60

The thermal parameters of decomposition processes of HL_1, L_2 along its Cu(II) complex, namely, activation energy (E_a), collision frequency (Z), enthalpy (ΔH), entropy (ΔS), and Gibbs free energy change (ΔG), were calculated by the Coats–Redfern method (Fouad *et al*., 2021) (Equation 1);

$$\log\left(\ln\frac{W_c/W_r}{T^2}\right) = \log\left(\frac{ZR}{\phi E_a}\left(1-\frac{2RT}{E_a}\right)\right) - \frac{E_a}{2.303RT} \qquad (1)$$

where$W_r = W_c - W$, W_c = mass-loss at the completion of reaction, W = mass-loss up to time ‘t’, Z = collision frequency, R = gas constant = 8.314 $J{\cdot}mol^{-1}{\cdot}K^{-1}$, E_a= energy of activation, T = temperature (K) and ϕ = heating rate = 0.166 s^{-1}.

Since $\frac{1-2RT}{E_a}$ is unity, a plot of $\log\left(ln\frac{W_c/_{W_r}}{T^2}\right) Vs \left(1/_T\right)$ will give a straight line, the slope of which is equal to $E_a/2.303R$ from which E_a and Z can be calculated using Equation (2).

$$\text{intercept} = \log\left(\frac{ZR}{\phi E_a}\right) \qquad (2)$$

where E_a = activation energy from graph

The kinetic and thermodynamics parameters obtained using Coats-Redfern plot are presented in Table 5. The values of activation energy (kjoules) obtained were 54.05, 25.59 and 25.95 for HL_1, L_2 and Cu(II) complex respectively. Due to the relatively small activation energy values, it can be shown that both the rate of decomposition and the "apparent" rate constant of the overall decomposition, as determined by Arrhenius behaviour increased with temperature. This suggests that there was no complicated mechanism involved in the ligand and metal complex breakdown. (Iorungwa *et al*., 2019) and the relatively higher E_a for HL_1 explains the extra energy needed by HL_1 and Cu(II) complex as compared to L_2 to undergo decomposition.

The collision frequency (Z) can be envisaged as the frequency of properly oriented collisions between reactant particles. It is possible to forecast the space or volume of the interacting molecules using the collision frequency values (Vyazovkin, 2021). The values of Z obtained in this study were 7.06×10^{16}, 4.01×10^{4} and 7.60×10^{4} for HL_1, L_2 and Cu(II) complex. These values illustrate that, more space or volume could be present in HL_1 and Cu(II) complex than in L_2 (Figures 7a-c). The values agree with the frequency of collision observed for the ligands and the Cu(II) complex. Theoretically, lowering the value of E_a leads to an increased collision frequency while an elevated value of E_a indicates higher stability (Wang *et al*., 2021).

For HL_1, L_2 and Cu(II) complex, enthalpy, ΔH, ($KJmol^{-1}$) were 50.25, 21.82 and 22.11, indicating that there was decomposition as energy was absorbed during the endothermic reaction. The enthalpy of HL_1 was higher, explaining that the total energy expended by HL_1 to split into the various components was more than the energy consumed by L_2. This could be attributed to the extra stability of HL_1, hence, requires greater amount of energy to break the chemical bond present in the ligand (Ohia *et al*., 2013).

The Gibbs free energy (ΔG) values are all positive (Table 6). The positive values show that the process required energy to occur, indicating a non-spontaneous process. The entropy value for HL_1 was 74.10 while L_2 and Cu(II) complex were found to be -160.29 and -156.60 kJoule respectively. The positive value of entropy for HL_1, indicates that the degree of disorderliness of the products formed through dissociation of bonds is higher than that of the reactants whereas the negative values of entropies for L_2 and Cu(II) complex, indicates that the degree of disorderliness of the products formed through dissociation of bonds is lower than that of the reactants.

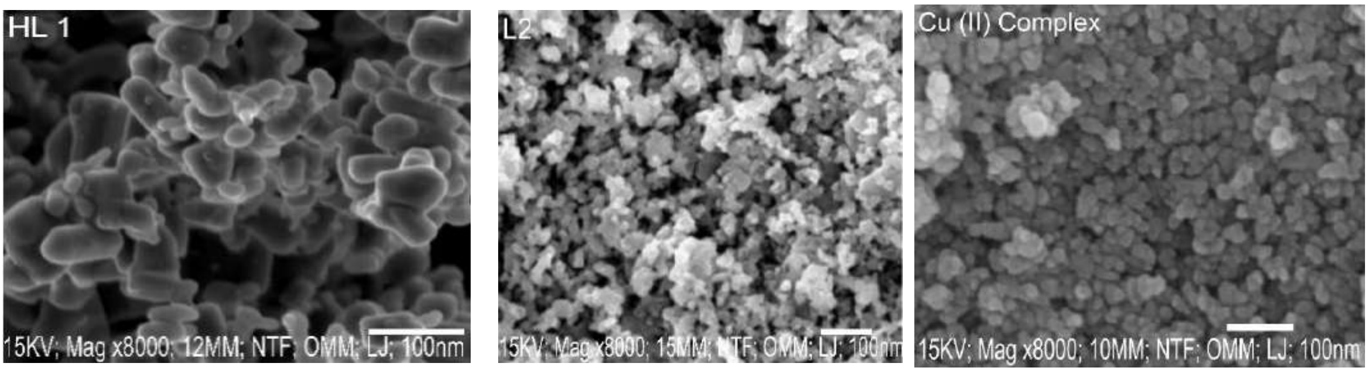

(a) **(b)** **(c)**

Figures 2a-c: The SEM Micrographs showing the Morphologies of HL$_1$, L$_2$ and its Cu(II) complex

Using scanning electron microscopy, the surface morphology of the metal complex was examined. In this study, SEM images were recorded at energy of 20 kV with magnification × 10000 to be used for imaging of the synthesized ligands and metal complex. Morphological analyses (texture, pores, and pore diameters) were also performed to ascertain whether complexation had occurred during grinding. The micrographs (Figures 2a-c) show the morphology of the ligands and the metal complex. By comparing these micrographs, it was possible to see that the ligand had formed complex with the metal salt and that a new product had developed, methodically filling the ligands' holes. The lowering of pore diameters and particle-particle interconnectivity was caused by the enhanced physical interconnection of the ligands and metal salt during complexation. The ligand micrograph's cross-sectional view shows the presence of several pores with diameters that are bigger than those seen in the metal complex micrograph. This shows that the porosity decreased during complexation as a result of the metal salts filling the ligands pores. (Zuehlsdorff and Isborn 2017). The SEM micrographs also showed changes in texture and morphology that accompanied the mixing of ligands and metal salt in the mortar-pestle grinding synthesis of the complex (Figure 2c**)**. The result shows that the particle shape and size changed throughout the complexation process.

Table 6: Diameter of Inhibition Zone of Microbes (nm) of the Synthesized Ligand with its Complex (50 and 100 mg/mL)

Ligands and its metal complex	***S. aureu***		***S. typhi***		***E. coli***		***M. canis***		***C. albican***		***T. rubbrum***	
	50	**100**	**50**	**100**	**50**	**100**	**50**	**100**	**50**	**100**	**50**	**100**
HL$_1$	9	11	8	9	8	9	11	11	12	14	**--**	**--**
L$_2$	15	17	10	12	13	14	9	10	12	14	**--**	**--**
Cu(II) Complex	21	23	20	21	18	20	15	16	21	23	15	17
Amoxicillin	32	34	28	30	26	28	--		--		--	
Nystatin	-	-	-	-	-	-	25	27	29	31	23	25

Observation	**Report**
Inhibition zone > 18 nm	Highly active
Inhibition zone > 12 nm	Moderately active
Inhibition zone > 7 nm	Slightly active
Inhibition zone = 7 nm	Inactive
--- (NA)	No activity (El-Barasi *et al.*, 2020)

The synthesized ligands and the Cu(II) complex were tested against bacterial and fungal strains by disc diffusion method. The microorganisms used in the present investigations included Gram-positive *Staphylococcus aureus* and *Staphylococcus typhi* bacterial strains, Gram-negative *Escherichia Coli.* Fungal strains were *Candida albicans*, *Microsporum canis* and *T. rubrum*. The results were compared with those of the standard drugs (amoxicilin for bacteria and nystatin for fungal). Results of the zones of inhibition measured for ligands (HL$_1$ and L$_2$) along its metal complex against the bacterial and fungal strains are presented (Table 6). Zones of inhibition showed that the ligand (HL$_1$) was slightly active against *S. aureus* (9, 11 nm), *S. typhi* (8, 9 nm), *E. coli* (8, 9 nm), *M.canis* (11, 11 nm) and moderately active against *C. albicans* (12, 14 nm) at a concentration of 100 mg/L but could not inhibit the growth of *Trichophytum rubrum.* However, L$_2$ was moderately active against *S. aureu*s (15, 17 nm), *E. coli* (13, 14 nm) and *C. albican* (12, 14 nm) at a concentration of 100 mg/L but was slightly active against *S. typhi* (10, 12 nm) and *Microsporum* *canis* (9, 10) and had no zone of inhibition against *Trichophytum rubrum.*

Cu(II) complex was highly active against all the tested microbes at both concentration of 50 and 100 mg/L except against *M. canis* (15, 16 nm) and *T. rubrum* (15, 17 nm) which it was moderately active. In comparison with amoxicilin and nystatin, HL_1 displayed less than 50 % inhibition against all test microbes at both concentrations of 50 and 100 mg/mL whereas L_2 displayed 50 % inhibition against *S. aureus* at a concentration of 100 mg/mL and *E. coli* at both concentrations of 50 and 100 mg/mL. This indicates its greater effectiveness against the microbes than HL_1 which could be attributed to some substituents present in $L_{1.}$ Cu(II) complex displayed more than 50 % inhibition against all the tested microbes as compared with the reference drugs. This enhanced inhibition of the complex can be explained in terms of the Tweedy's chelation theory (Pahontu *et al*., 2015). Due to the ligand's orbital overlap and the metal ion's partial sharing of its positive charge with donor groups during the formation of the metal complex, the polarity of the metal ion was greatly lowered. Moreover, delocalization of the π-electrons over the whole chelate was enhanced (Siguh and Chaudhary, 2004). As a result of these characteristics, the complex was able to more easily pass through the microbe's membrane and DNA, disrupting their respiration process and preventing protein synthesis, which prevented the microorganisms from growing any further. This could therefore, in severe circumstances, cause the impacted bacteria to die (Siguh and Chaudhary, 2004).

CONCLUSION

Grinding as a solvent-free synthetic method was applied to synthesise ligands HL_1 and L_2 with their Cu(II) complex. The ligands and the complex were characterized and tested for their antimicrobial activities. The solubility result of the ligand and the complex revealed their non polarity which was affirmed by molar conductivity results as non-electrolytes. The IR spectra showed that chelation of Cu(II) ion was through the deprotonated hydroxyl group and the azomethine nitrogen thus indicating the bidentate nature of the two ligands. Comparing the electronic spectra of the free ligands with that of the complex showed shift from lower to higher frequencies which confirmed the chelation of the two ligands and the metal ion. Results from ligands thermogravimetric analysis revealed the absence of water crystals while the metal complex contained crystals of water. In comparison to L_2 and Cu(II) complex, HL_1 required more energy to create an activated complex, as indicated by the activation energy which was determined by thermal analysis. This finding was further supported by the results of the collision frequency study. The ligands and the metal complex positive Gibb's free energy (ΔG) values indicate a non-spontaneous process. The positive and negative values of entropy indicate that the degree of disorderliness of the products formed by the dissociations of the bonds is higher or lower than that of the initial reactants. The antimicrobial studies revealed that the ligands were moderately active against all the test microbes but not on *T. rubrum*, the metal complex showed significantly enhanced activity against the studied microbes when compared with the free ligands. An increase in concentration closely correlated with their efficacy as antibacterial agents. In comparison to standard drugs, their activities suggest that the ligands and metal complex are potential control agents that could be used in an integrated program to manage bacteria and fungi.

REFERENCES

Adkis, A., Benali-Baitich, O., Khan, M. A. and Bouet, G. (2000). Synthesis, characterization and the thermal behaviour of mixed ligand complexes of cobalt(III) with dimethylgloxime and some amino acids. *Synthesis and Reactions in Inorganic Metals Organometallic and Nanomaterial Chemistry*, 30: 1849-1858.

Anitha, C., Sumathi, S., Tharmaraj, p.and sheela, C.D. (2011). Synthesis, characterization, and biological activities of some transition metal complexes derived from a novel Hydrazone Azo Schiff base ligand. International journal of inorganic, 9: 1 -12

Aiyelabola, T., Akinkunmi, E., Obuotor, E., Olawuni, I., Isabirye, D. and Jordaan, J. (2017). Synthesis, characterization and biological activities of coordination compounds of 4-hydroxy-3-nitro-2H-chromen-2-one and its aminoethanoic acid and pyrrolidine-2-carboxylic acid mixed ligand complexes. *Bioinorganic Chemistry and Applications*, 1155: 6426747.

Das, K. K., Reddy, R. C., Bagoji, I. B., Das, S., Bagali, S., Mullur, L., Khodnapur, J. P. and Biradar, M. S. (2019). Primary concept of nickel toxicity – an overview. *Journal of Basic Clinical, Physiological and Pharmacology*, 30(2): 141–152.

Doğan, S., Tümay, S. O., Balci, C., Yeşilot, S. and Beşli, S. (2020). Synthesis of new cyclotriphosphazene derivatives bearing Schiff bases and their thermal and absorbance properties. *Turkish Journal of Chemistry*, 44(1): 31 – 47.

Emiola-Sadiq, T., Zhang, L. and Dalai, A. K. (2021). Thermal and kinetic studies on biomass degradation *via* thermogravimetric analysis: A combination of model-fitting and model-free approach. *ACS Omega*, 6: 22233-22247.

Fouad, R., Shaaban, I. A., Ali, T. E., Assiri, M. A. and Shenouda, S. S. (2021). Co(II), Ni(II), Cu(II) and Cd(II)-thiocarbonohydrazonecomplexes: spectroscopic, DFT, thermal, andelectrical conductivity studies. *Royal Society of Chemistry Advances*, 11: 37726-37743.

Iniama, G. E., Iorkpiligh, T. I. & Essien, B. P. (2018). Synthesis, characterization, antibacterial and antifungal activities of Co(II), Ni(II) and Cu(II) Schiff base complexes derived from methionine and salicylaldehyde. *Chemistry Research Journal*, 3(3): 34-39.

Iorungwa, M. S., Wuana, R. A. & Dafa, S. T. (2019). Synthesis, characterization, kinetics, c and antimicrobial studies of Fe(III), Cu(II), Zn(II) N,N'-Bis(2-hydroxy-1,2-diphenylethanone)ethylenediamine complexes.*Chemical Methodologies*, 3: 408-424.

Kumar, S., Pandey, P. K., Sinha, N., Chaudhari, S. &Sharma, S. (2018). Spectroscopic characterisation of metal complexes with tetradentate ligand. *Journal of Physical Science*,29(3): 1–11.

Liu S., Elouarzaki, K. and Xu, Z. J. (2022). Electrochemistry in magnetic fields. *Angewandtei*, 61 (27): e202203564.

Mkpenie, V. N., Essien, E. E. & Mkpenie, I. V. (2015). Antimicrobial activity of azo-Schiff bases derived from salicylaldehyde and para-substituted aniline. *World Journal of Pharmaceutical Research*, 4(12): 52-60.

Moellering, R. C. (2011). Discovering new antimicrobial agents. *International Journal of Antimicrobial Agents*, 37 (1): 2-9.

Ohia, G. N., Amasiatu, G. I. & Ajagbe, J.O. (2013). *Comprehensive certificate chemistry. 2nd edition*. University press Pp. 218-219.

Ommenya, F.K., Nyawade, D.M. and Kinyua, J. (2020). Synthesis, characterization and antibacterial activity of Schiffbase, 4-chloro-2-{(E)-[(4 flurophenyl)imino]methyl}phenol metal (II) complexes. *Journal of Chemistry*, 2020: 1-8.

Patel, R. N., Singh, N., Shukla, K.K. Gundla, V.L.N. and Chauhan, U.K.(2006). Synthesis, characterization, and biological activity of ternary copper(II) complexes containing polypyridyl ligands. *Spectrochimica Acta, part A*, 6: 21-26.

Pointillart, F., Speed, S., Lefeuvre, B., Riobé, F., Golhen, S., Le-Guennic, B., Cador, O., Olivier M. O. & Lahcène Ouahab, L. (2015). Magnetic and photo-physical properties of lanthanide dinuclear complexes involving the 4,5-bis(2-pyridyl-n-oxidemethylthio)-4′,5′-dicarboxylic acid-tetrathiafulvalene, dimethyl ester ligand. *Inorganics*, 3(1): 554-572.

Salvaganapathy, M .and Raman, N. (2016). Pharmacological activity of few transition metal complexes: A short Review. *Journal of Chemical Biology and Therapeutic*, 1: 1-10

Slavin, Y. N., Asnis, J., Hafeli, U.O. and Bach, H. (2017). Metal Nanoparticles: understanding the mechanisms behind Antibacterial Activity. *Journal of nanobiotechnology*, 15: 1 – 20

Subin, K. and Aravindakshan, K. (2017). Synthesis, characterization, antimicrobial and antioxidant studies of complexes of Fe(III), Ni(II) and Cu(II) with novel Schiff base ligand (E)-ethyl 3-((2-aminoethyl)imino)butanoate. *Journal of Pharmaceutical, Chemical and Biological Sciences*, 5(3): 177-186.

Terreni, M., Taccani, M. and Pregnolato, M. (2021). New antibiotics for multidrug-resistant bacterial strains: latest research developments and future perspectives. *Molecules*, 26 (9): 26-71

Wang, Z., He, J., Li, Q., Tang, Y., Wang, J., Pan, Z., Chen, X. and Jiao, X. (2020). First Detection of NDM-5-Positive Salmonella Enterica Serovar Typhimurium Isolated from Retail Pork in China. Microb. *Drug Resistant Larchmot*, 26: 434-437.

Zuehlsdorff, T. J and Isborn, C. M.(2017). Combining the ensemble and Franck-Condon approaches for calculating spectral shapes of molecules in solution. *The Journal of chemical science*, 148(1): 1-17.